frontiers | Frontiers in Earth Science

TYPE Original Research
PUBLISHED 25 October 2024
DOI 10.3389/feart.2024.1405768

OPEN ACCESS

EDITED BY
Florentin Maurrasse,
Florida International University, United States

REVIEWED BY
Luigi Jovane,
University of São Paulo, Brazil
Andrej Spiridonov,
Vilnius University, Lithuania

*CORRESPONDENCE
Mihaela Melinte-Dobrinescu,
melinte@geoecomar.ro

RECEIVED 23 March 2024
ACCEPTED 29 August 2024
PUBLISHED 25 October 2024

CITATION
Melinte-Dobrinescu M, Chen X, Anton E, Apotrosoaei V and Yao H (2024) Calcareous nannoplankton fluctuation within the Albian-Cenomanian Boundary Event of the Tethyan Himalaya.
Front. Earth Sci. 12:1405768.
doi: 10.3389/feart.2024.1405768

Calcareous nannoplankton fluctuation within the Albian-Cenomanian Boundary Event of the Tethyan Himalaya

Mihaela Melinte-Dobrinescu[1,2]*, Xi Chen[3], Eliza Anton[1], Vlad Apotrosoaei[1,2] and Hanwei Yao[3]

[1]National Institute of Marine Geology and Geo-Ecology, Bucharest, Romania, [2]Doctoral School of Geology, University of Bucharest, Bucharest, Romania, [3]State Key Laboratory of Bio-Geology and Environmental Geology, China University of Geosciences, Beijing, China

A hemipelagic succession 29m thick, situated in South Tibet within the Tethyan Himalaya tectonic unit, has been investigated for its calcareous nannofossil content. A total of 17 samples were subject to qualitative and semi-quantitative analysis. The studied interval belongs to the upper Albian-lowermost Cenomanian and extends into the UC0 nannofossil zone; based on the last occurrence of *Hayesites albiensis*, the UC0a and UC0b-c subzones were recognized. The most abundant nannofossil of the Youxia section is *Watznaueria barnesiae*. Other common taxa are *Eiffellithus turriseiffelii*, *Eprolithus floralis, Rhagodiscus* spp., and *Zeugrhabdotus* spp. In the lowermost part of the studied section, below the beginning of the Albian-Cenomanian Boundary Event (ACBE), i.e., prior to the $\delta^{13}C$ positive excursion related to OAE1d, the nannofossils confined to high paleolatitudes, namely *Repagulum parvidentatum*, *Seribiscutum primitivum*, and *Sollasites horticus*, are present with a low abundance. This occurrence is believed to be evidence of a short episode of cooler surface waters linked to a transgressive event. The nannofossil abundance and diversity, along with the fluctuation patterns of the nutrient and temperature indices throughout the section, reflects a primary signal of mesotrophic to eutrophic conditions from the base of the succession up to the two oldest $\delta^{13}C$ peaks of ACBE, both late Albian in age and within the OAE1d. By contrast, the dominance of *Watznaueria barnesiae*, representing more than 80% of the total assemblages, along with the significant drop in abundance and diversity shown by nannofossils within late phases of ACBE, are interpreted as a diagenetic signal. Mesotrophic to eutrophic conditions returned towards the top of the studied succession, where *Biscutum constans* and *Zeugrhabdotus erectus* again show a higher abundance.

KEYWORDS

late Albian-early Cenomanian, Oceanic anoxic event 1d, nannofossils, South Tibet

1 Introduction

The Oceanic Anoxic Events (OAEs) represent major disturbances in the global carbon cycle, covering episodes of widespread marine anoxia and major oxygen depletion in the marine realm. During the setting of an OAE, biogeochemical cycles are modified and are linked to major changes in the ocean and atmosphere of the Earth (i.e.,Schlanger and Jenkyns, 1976; Jenkyns, 1980; Arthur et al., 1988; Kuypers et al., 1999; Bodin et al., 2010; Kemp et al., 2022).

Several changes took place during the setting of an OAE, such as the shift of $\delta^{13}C$ isotope values, changes in lithology, including the occurrence of rich-organic black shales in deep-marine deposits, and modifications of biotic assemblages, especially marine planktonic ones, which are more sensitive to environmental changes (i.e., Arthur and Premoli-Silva, 1982; Jenkyns and Clayton, 1986; Mutterlose and Kessels, 2000; Leckie et al., 2002; Herrle et al., 2003; Erba et al., 2004; Dumitrescu and Brassels, 2006; Cohen et al., 2007; Jenkyns et al., 2017).

A rapid global warming during the setting of OAEs was described by numerous publications (e.g., McAnena et al., 2013; Bottini et al., 2015; Huber et al., 2018). Increased temperature values and the higher hydrological regime (Menegatti et al., 1998; Bodin et al., 2015) led to increased primary productivity, causing anoxic oceanic conditions. Most probably, the high volcanogenic CO_2 content in the Earth's atmosphere was the main factor leading to the development of the greenhouse climate, also implying continental weathering and higher nutrient content brought by rivers (Föllmi et al., 1994; Erba and Tremolada, 2004; Turgeon and Brumsack, 2006). Additionally, the idea of the global ocean enhancing fertility is possibly linked to the huge amount of biolimiting metals produced by submarine igneous events (Erba, 2004; Weissert and Erba, 2004). The mid-Cretaceous times are characterized by the occurrence of the most numerous Oceanic Anoxic Events (OAEs) in the whole Mesozoic (i.e., Schlanger and Jenkyns, 1976; Jenkyns, 2010). Most of these OAEs probably reflect the presence of superplumes, associated with high ocean crust formation rates and increased volcanism (Arthur et al., 1985; Larson, 1991; Larson and Erba, 1999; Wilson and Norris, 2001; Friedrich et al., 2012). Based on isotopic investigations of Cretaceous OAEs, important changes in the global carbon cycle were reported, especially within the Aptian-early Turonian interval (Jenkyns et al., 1994; Mitchell et al., 1996; Jenkyns, 2010; Richey et al., 2018; Sames et al., 2016; Yao et al., 2021).

One of the most significant disturbances of the carbon cycle produced in the mid Cretaceous was discovered within the Albian-Cenomanian boundary interval, namely, the Albian-Cenomanian Boundary Event (ACBE). This event is characterized by the presence of four successive peaks (A, B, C, and D) identified by Gale et al. (1996) in Southeast France (the Vocontian Basin), based on the $\delta^{13}C$ isotope positive excursion. The oldest Albian peak is described as the OAE1d (Jarvis et al., 2006; Gale et al., 2011), known as the Breistroffer Event in SE France (Breistroffer and Hebd, 1937; Bréhéret, 1997; Giraud et al., 2003; Bornemann et al., 2005) and the Pialli level in the Italian Apennines (Coccioni et al., 2006). This chemostratigraphic event was revealed in many Tethyan successions (western equatorial Atlantic–Petrizzo et al., 2008; NW Turkey; Yilmaz, 2008; N Tunis–Fahdel et al., 2011; New Mexico, United StatesScott et al., 2013; Eastern Carpathians–Melinte-Dobrinescu et al., 2015; Tibet–Yao et al., 2018; Yao et al., 2021; Wang et al., 2022; Poland–Górny et al., 2022; Bąk et al., 2023; Egypt–Mansour and Wagreich, 2024, among others), in Boreal ones (i.e., Speeton, United Kingdom - Mitchell et al., 1996; Hanover area, N Germany - Bornemann et al., 2017), and also higher southern latitudes (>60°), according to Fan et al. (2022). The widespread occurrence of the chemostratigraphic signature indicates that the ACBE, including the lower part (OAE1d), might be regarded as a globally distributed oceanic anoxic event.

As with other planktonic marine organisms, the calcareous nannoplankton group is very sensitive to surface water changes, such as temperature, pH, nutrient input, salinity, and dissolved CO_2. Linked to the OAE occurrence, the nannofossils show a turnover, i.e., either a speciation event preceding the OAE or an extinction event followed by speciation, and a temporary disappearance of high-fertility proxies (i.e., Lamolda et al., 1994; Erba, 2004; Linnert et al., 2010; Fahdel et al., 2011; Melinte-Dobrinescu et al., 2013; Aguado et al., 2016). Some authors assume that, within the latest Albian, there are minor modifications in surface water fertility (Giraud et al., 2003), probably reflecting changes from mesotrophic to more oligotrophic conditions (Erba and Tremolada, 2004; Bornemann and Mutterlose, 2006; Mutterlose et al., 2022) linked to climatic variations. The findings from Bornemann et al. (2005) are indicative of reduced surface water productivity during the black shale deposition of OAE1d in the Vocontian basin, France. In the Northwest African Margin, Chin and Watkins (2019) identified fluctuations in surface water productivity within ACBE and lower Cenomanian Events I to III, based on modifications in nannofossil assemblages, especially on increased abundance of *Biscutum* spp. at the onset of the above-mentioned anoxic events, accompanied by a shift in the Shannon diversity index.

The present study aims to use the calcareous nannofossil distribution pattern in the Youxia section, South Tibet, to constrain the ACBE, whose lower part includes OAE1d. We present the results of the qualitative and semi-quantitative calcareous nannofossil investigations, the shift of isotope $\delta^{13}C$ values, and the relationship between nannofossil abundance and diversity. Implications for the generation of the ACBE in the eastern Tethyan Realm are also discussed.

2 Geological background

The studied Youxia section is situated in S Tibet (Figure 1A), a region comprising five tectonic units: the Higher Himalayan Crystalline Belt, the Tethyan Himalaya tectonic zone, the Indus-Yarlung Zangbo suture, the Xigaze forearc basin, and the Gandese Arc (Gansser, 1991). Cretaceous marine deposits in southern Tibet are mainly exposed in the Tethyan Himalaya tectonic unit and were emplaced in the Northern Indian microcontinent during Early Cretaceous times (Hu et al., 2010).

According to Patzelt et al. (1996), the study area was located at the 21°S paleolatitude during the mid Cretaceous (Figure 1C), connecting the Pacific with South Tethys (Scotese, 1991; 2021). In the Tingri area of the Tethyan Himalaya tectonic unit, Cretaceous successions comprise hemipelagic sediments up to 600m thick, mainly composed of marls and limestones and some clays (Willems et al., 1996).

3 Materials and methods

The Youxia section, S Tibet, is 140 m-thick. The whole succession, as published by Yao et al. (2018), extends within the upper Albian-lower Turonian interval, encompassing the UC0 up to UC6 nannofossil zones of Burnett (1998).

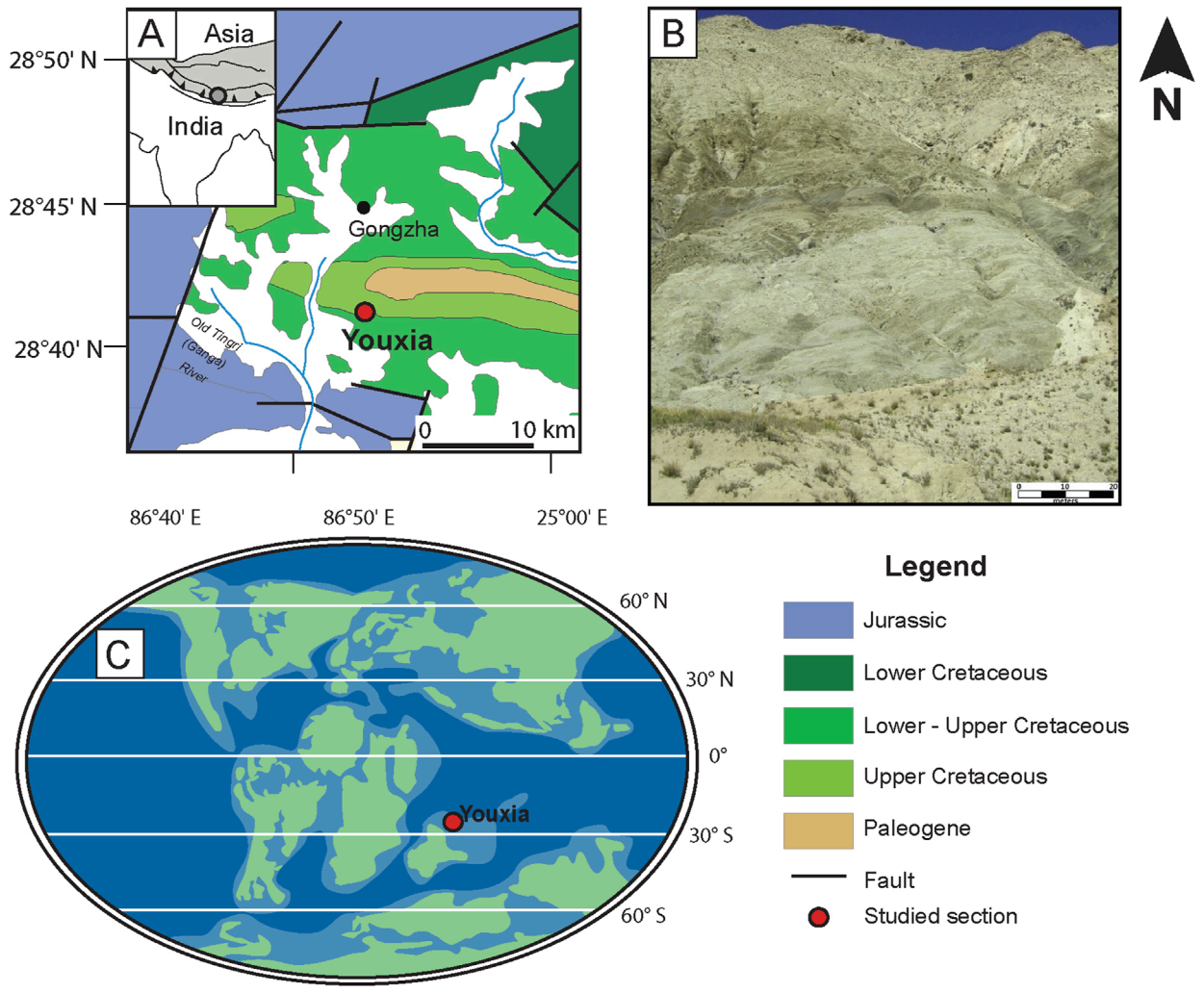

FIGURE 1
(A) Location of the studied sections Youxia section, Tingri area, S Tibet (after Hu et al., 2010; Yao et al., 2018): **(B)** Photograph of the studied section (from Yao et al., 2018). **(C)** Paleogeographic setting of Youxia section (21°S), late Albian (around 100 Ma) paleogeography (after Hay, 2009; Scotese, 1991; 2021).

The lower part of the studied section, between 0 and 29 m, namely, the Lengqingre Formation of the Gamba Group, spans the upper Albian–lowermost Cenomanian. The 29 m thick (Figure 1B) succession, subject of this work, is composed of grey calcareous shales, interbedded with whitish marlstones and limestones (Li et al., 2006; Yao et al., 2018).

We performed qualitative and semi-quantitative analyses of 17 calcareous nannofossil samples. Nannofossil assemblages were studied under a polarizing light microscope at ×1,250 magnification; smear slides were prepared using standard techniques (Bown and Young, 1998). The given diversity represents the total number of encountered taxa in each sample, while the abundance was calculated as the average number of specimens found in LM fields of view. In total, 250 nannofossil specimens were counted/sample. The first occurrence (FO) was used for the lowest stratigraphic occurrence of a species identified in the section, while the last occurrence (LO) was used for the highest stratigraphic occurrence of a taxon.

We calculated the nutrient index (NI) and the temperature index (TI), which are useful for highlighting paleoecological changes based on calcareous nannofossils (Herrle and Mutterlose, 2003; Tiraboschi et al., 2009; Bottini et al., 2015; Aguado et al., 2016).

We have used the TI and NI of Herrle et al. (2003), partly modified by excluding taxa that discontinuously occurred and show a low abundance in the Youxia section.

$$NI = (\text{high fertility taxa}/\text{high fertility taxa} + \text{low fertility}) * 100$$

In the high fertility nannofossil group, we have included *Biscutum constans*, *Discorhabdus ignotus*, and *Zeugrhabdotus erectus*, while the low fertility nannofossil group consists only of *Watznaueria barnesiae*, in agreement with previous studies, e.g., Mutterlose (1992a), Erba (2004), Lees et al. (2005), Mutterlose et al. (2005), and Bornemann et al. (2005).

$$TI = (\text{warmer surface} - \text{water taxa}/\text{warmer surface} - \text{water taxa} + \text{cooler surface} - \text{water taxa}) * 100$$

For the warmer-temperature surface water nannofossils, we included the species *Rhagodiscus asper*, *Nannoconus* spp., *Hayesites albiensis*, and *Zeugrhabdotus diplogrammus*, while the cooler-temperature surface water group comprises *Eprolithus floralis*, *Repagulum parvidentatum, Sollasites horticus,* and *Seribiscutum primitivum* (Roth and Krumbach, 1986; Erba et al., 1992; Mutterlose, 1992a; 1992b; Herrle and Mutterlose, 2003; Herrle et al., 2003; Tiraboschi et al., 2009; Bottini and Erba, 2018).

4 Results

4.1 Calcareous nannofossil assemblages

In total, 59 nannofossil taxa were identified. The diversity varies between 15 and 44; the highest values were encountered in the lower part of the studied succession (between 0 and 1.9 m), within the upper Albian, up to the base of the oldest $\delta^{13}C$ positive excursion described in the section by Yao et al. (2018), while the minimum is situated in the lower Cenomanian, above the end of the ACBE (15.7–18.3 m). The most abundant species is *W. barnesiae*, with an abundance over 80% in the middle part of the studied section (i.e., 14.8–18.3 m) and lower values up to 38.4% towards the base (between 0 and 2.8 m) and topmost area (i.e., 25.2–29 m) of the studied succession.

Commonly encountered nannofossils were *Eiffellithus turriseiffelii* (between 5.1% and 9.8%), *E. floralis* (from 8.7 up to 19.8%), and *R. asper* (between 5.9% and 18.7%). There was consistent occurrence of the genera *Eiffellithus* (mainly *E. turriseiffelii* and *E. gorkae* in a small amount), *Rhagodiscus* (*R. achylostaurion*, *R. asper*, *R. angustus*, *R. infinitus*, and *R. splendens*), and *Zeugrhabdotus* (*Z. diplogrammus*, *Zeugrhabdotus embergeri*, and *Z. erectus*) (Supplementary Table S1, Figures 2, 3).

Cretarhabdus spp., *Broinsonia enormis*, *Prediscosphaera columnata*, and *Tranolithus orionatus* occured continuously throughout the studied succession but with low abundances. *Amphizygus brooksii*, *Bukrylithus ambiguus*, and *Lithraphidites* (*Lithraphidites carniolensis* and *Lithraphidites alatus*), along with *Microrhabdulus*, *Radiolithus*, *Retecapsa*, and *Staurolithites* genera, appear discontinuously and with a low abundance (each between 0.4% and 1.2% of total assemblages). The genus *Braarudosphaera* (*B. bigelowii* and *B. hockwoldensis*) sporadically occur in the Youxia section (Figure 4), except for a short interval (between 9.2 and 15.3 m) where the two species jointly make up to 15%. The nannoconids are mainly represented by *Nannoconus truittii*, showing a peak of 5.5% at 8.9 m.

Repagulum parvidentatum is present between 0 and 2.8 m and represents up to 2.8% of the nannofossil assemblages. In the same samples, *S. horticus* and *S. primitivum* are present, each representing less than 1% of total assemblages, whereas *Biscutum constans* and *Z. erectus* display higher abundances, between 7.5% and 5.8%.

4.2 Calcareous nannofossil biostratigraphy

The biostratigraphy of the studied Youxia succession follows the work of Yao et al. (2018), who studied an extended interval of this section. According to their work, the interval presented in this paper, between 0 and 29 m, is covered by the UC0 biozone of Burnett (1998). Based on the LO of *H. albiensis*, Yao et al. (2018) identified the boundary between the UC0a and UC0b-c subzones of Burnett (1998). The boundary between UC0b and UC0c subzones was not identified, as *Calculites anfractus* is not present. Yao et al. (2018) reported the successive LOs of *Cylindralithus serratus* and *Gartnerago chiasta* within the UC0b-c subzones.

The UC0a subzone was assigned based on the co-occurrence of *E. turriseiffelii*, *Axopodorhabdus albianus, L. alatus*, *T. orionatus*, and *H. albiensis* (Supplementary Table S1), all of them with their FO in the Albian stage (Applegate and Bergen, 1988; Bown et al., 1998; Burnett, 1998; Gale et al., 2011). Additionally, *Crucicribrum anglicum*, a nannofossil ranging in the middle to upper Albian (Jeremiah, 1996; Bown, 2001), is present from the base of the investigated succession and disappears towards the top of UC0a, 1.2 m below the LO of *H. albiensis* (Figure 2).

The boundary between the Albian and Cenomanian stages falls within the upper part of the UC0 biozone (Burnett, 1998; Kennedy et al., 2004; Gale et al., 2011). The same biostratigraphic position of the Albian-Cenomanian boundary, at the upper part of the UC0 biozone, within the UC0b-c subzones, was also considered in the Youxia section. Based on the $\delta^{13}C$ isotope fluctuation of the studied succession, the Albian-Cenomanian boundary is placed between peaks C and D (Yao et al., 2018), the same as at the GSSP of the base of the Cenomanian stage at Mont Risou, France (Gale et., 1996; Kennedy et al., 2004) and other Tethyan sections, such as Monte Petrano, Italy (Gambacorta et al., 2015) and Black Noise, Northwest Atlantic (Wilson and Norris, 2001).

4.3 Calcareous nannofossil preservation

The preservation state throughout the studied section is moderate, as specimens show little effects of secondary alteration from etching and/or overgrowth, allowing the identification at a specific level of up to 70% of specimens. The lower and upper parts of the studied section, between 0–7.9 m and 22.8–29 m respectively, contain nannofossils that could be considered prone to dissolution (i.e., Leckie et al., 2002; Erba, 2004; Lees et al., 2005; Mutterlose et al., 2005), such as *Biscutum constans*, *D. ignotus,* and *Z. erectus*. In the middle part of the section, between 7.9 and 22.8 m, during the latest phases of the ACBE, *D. ignotus* and *Z. erectus* disappeared, while *Biscutum constans* shows a low abundance, less than 1%, coeval with the significant increase over 80% of *W. barnesiae* (Figure 2).

Previous studies (Roth and Krumbach, 1986; Bruno et al., 2022) suggested that a high abundance of *W. barnesiae*, i.e., over 40% of total assemblages, implies a significant impact of the diagenetic processes. In general, *W. barnesiae* is regarded as a cosmopolitan species, able to adapt more efficiently than other nannofossils to environmental fluctuations (Mutterlose, 1992a; Mutterlose, 1992b; Street and Bown, 2000; Aguado et al., 2016) such as temperature, pH, and salinity. This taxon could be regarded as a Cretaceous equivalent of the extant *Emiliania huxleyi* (Melinte and Mutterlose, 2001), being an ecologically robust species able to settle in new biotopes. Nowadays, *E. huxleyi* is present globally in marine settings, with a salinity ranging between 11‰ (in the Black Sea) and 42‰ (the Red Sea), both in shallow- and deep-marine environments (Bukry, 1974; Giunta et al., 2007; Ion et al., 2022, among others). We suppose a similar distribution pattern for *W. barnesiae* during Cretaceous times.

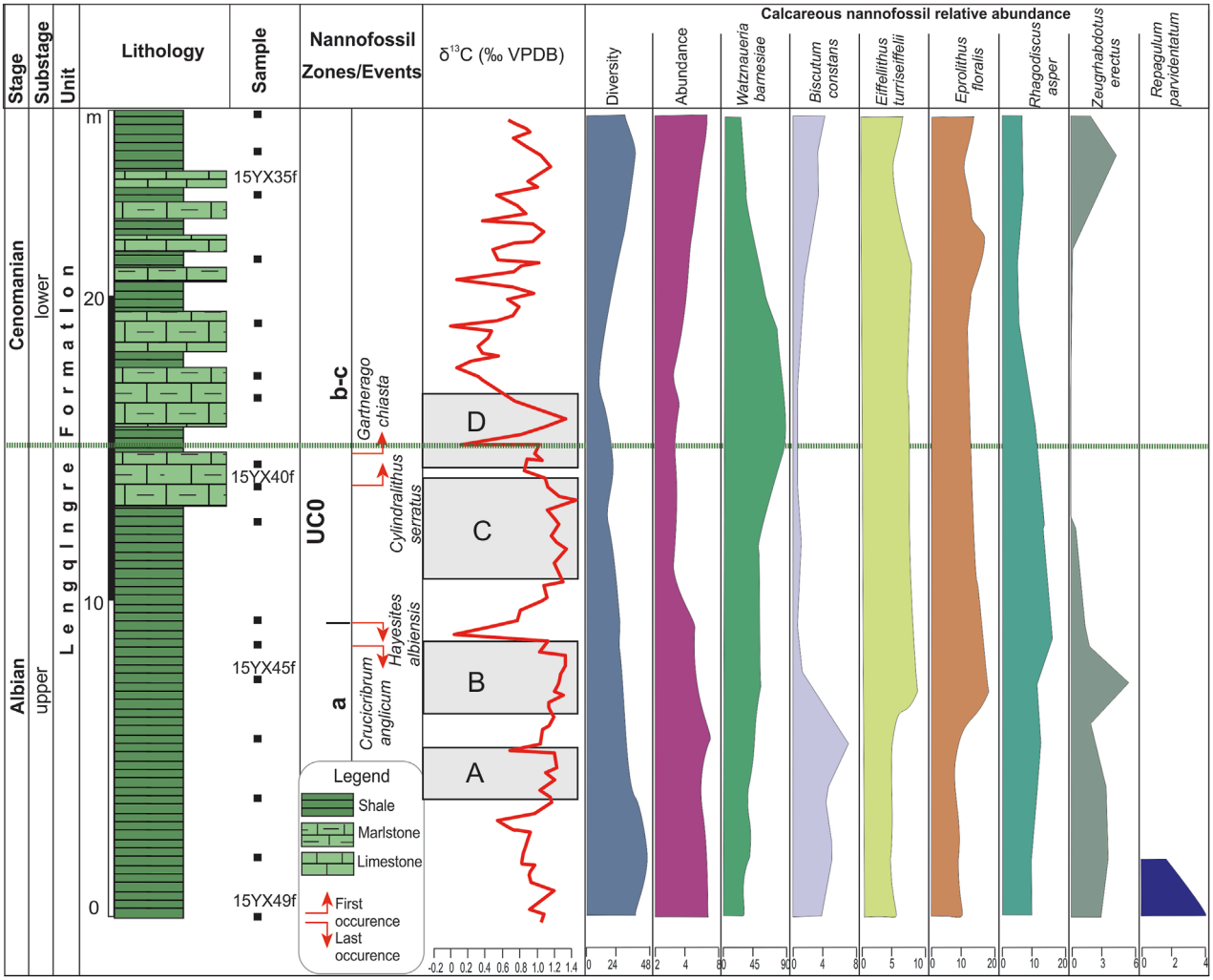

FIGURE 2
Calcareous nannofossil relative abundance across the Albian-Cenomanian Boundary Interval of the Youxia section (S Tibet). Lithology and $\delta^{13}C$ isotope fluctuation after Yao et al. (2018).

In the studied succession, *W. barnesiae* peaks are well correlated with increased values of $\delta^{13}C$ in the late phases C and D of ACBE and show a negative correlation with the diversity and abundance of nannofossil species (Figure 2). Therefore, we may assume that the original calcareous nannofossil assemblage composition is significantly altered between 7.9 and 22.8 m, during the latest phases of the ACBE.

5 Discussion

5.1 Nannofossil and $\delta^{13}C$ fluctuations related to the Albian-Cenomanian boundary event

The isotope $\delta^{13}C$ values indicate noticeable fluctuations throughout the upper Albian - lower Cenomanian interval of the studied succession, from 0‰ up to +1.3‰, displaying four distinct positive excursions. Peak A (OAE1d) and peak B in the late Albian are the oldest $\delta^{13}C$ positive excursions, peak C is the latest Albian to earliest Cenomanian in age, and peak D is earliest Cenomanian (Yao et al., 2018; Yao et al., 2021).

In the interval covered by peak A of $\delta^{13}C$, the nannofossil assemblages are similar in abundance, diversity, and composition to the ones identified in the lower interval, i.e., from the base of the section up to 2.9 m. The only difference is the disappearance of the taxa mostly confined from middle-to high paleolatitudes (Supplementary Table S1), such as *R. parvidentatum*, *S. primitivum*, and *S. horticus*, coeval with increased abundance of high-fertility proxies *Biscutum constans* and *Z. erectus*.

Yao et al. (2021) identified a distinctive rise in Hg values right before the onset of OAE1d (below peak A), followed by another increase within the OAE1d, e.g., over peak A. The authors observed the absence of any correlation among Hg, organic matter (OM), Mn-Fe-oxyhydroxides, and clay mineral

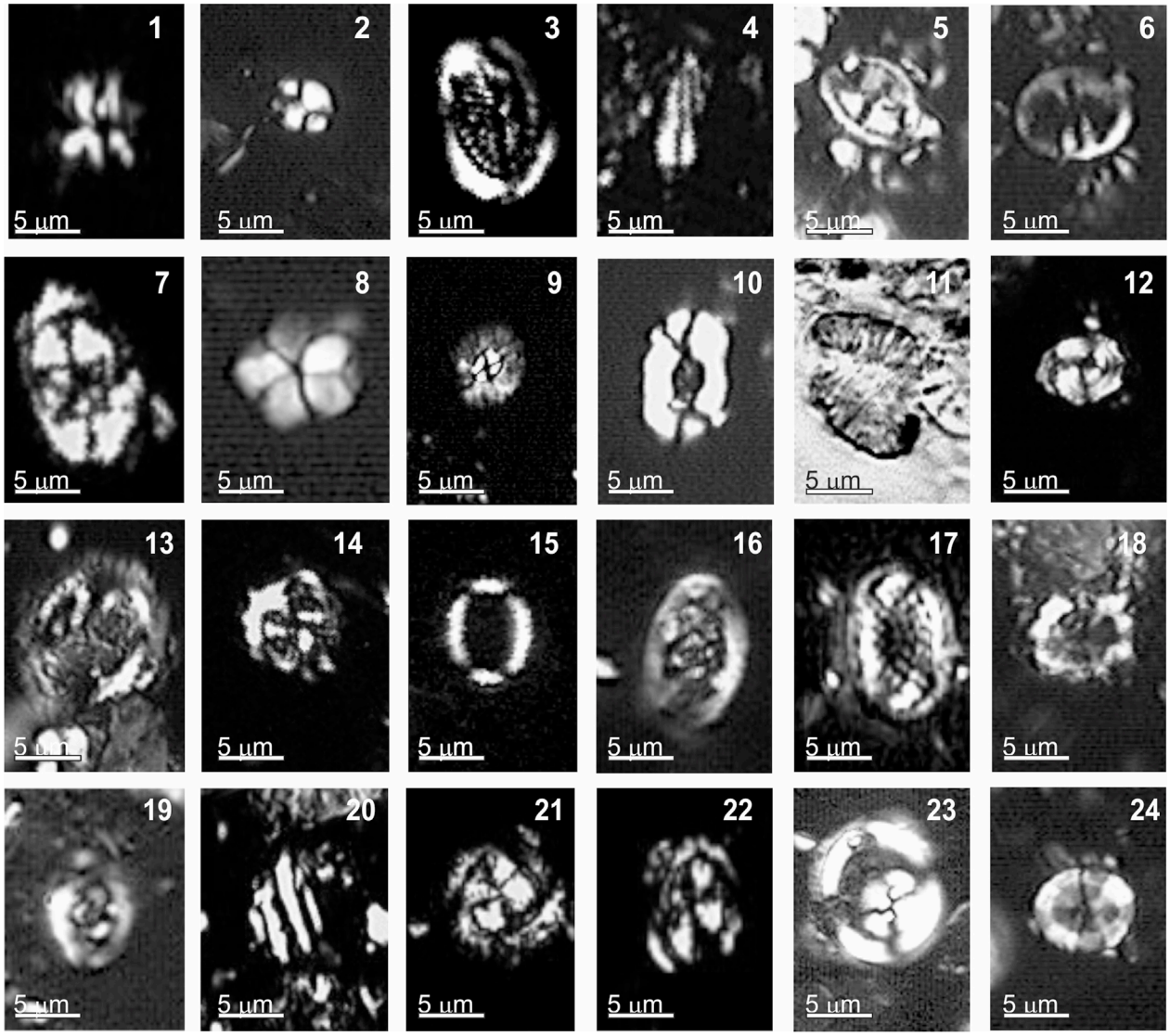

FIGURE 3
Calcareous nannofossil microphotographs of identified taxa in the Youxia section across the Albian-Cenomanian Boundary Event. LM (light microscope), N+ (crossed-nicols), except 10 in NII (polarized light). **1** – *Hayesites albiensis*; Sample 43. **2** – *Calculites percernis*; Sample 45. **3** – *Cretarhabdus striatus*; Sample 33. **4** – *Lithraphidites alatus*; Sample 34. **5** – *Tranolithus orionatus*; Sample 33. **6**–*Tranolithus orionatus*; Sample 49. **7**–*Eiffellithus turriseiffelii*; Sample 49. **8** – *Braarudosphaera hockwoldensis*; Sample 33. **9** – *Biscutum constans*; Sample 34. **10** – *Manivitella pemmatoidea*, inside *Watznaueria barnesiae*; Sample 33. 11 - *Nannoconus truittii*; Sample 33. **12** – *Cylindralithus serratus*; Sample 39. **13** – *Axopodorhabdus albianus*; Sample 49. **14** – *Gartnerago chiasta*; Sample 35. **15** – *Repagulum parvidentatum*; Sample 49. **16** – *Rhagodiscus asper*; Sample 33; **17** – *Cribrosphaerella ehrenbergii*; Sample 33. **18** – *Eprolithus floralis*; Sample 33. **19** – *Helenea chiastia*; Sample 33; **20** – *Calcicalathina alta*; Sample 41. **21** – *Crucicribrum anglicum*; Sample 48. **22** – *Crucicribrum anglicum*; Sample 47. **23** – *Manivitella pemmatoidea*, inside *Watznaueria barnesiae*; Sample 43. **24** – *Radiolithus hollandicus*; Sample 36.

content. Thus, this pattern might be indicative of a volcanic origin rather than enhanced organic matter and/or increased run-off, an assumption that supports Large Igneous Province (LIP) volcanism prior to the onset of ACBE (i.e., OAE 1d). Since the Kerguelen LIP accounts for the longest, high-magma-flux emplacement interval of any LIP, associated with a high submarine volcanic activity and being the closest LIP to the study area (i.e., Frey et al., 2000; Jiang et al., 2021 and references herein), we may hypothesize that the increased abundance of nannofossil high-fertility surface water proxies is mainly related to a considerable flux of biolimiting metals produced during submarine igneous events.

Watznaueria barnesiae shows high percentages (over 80%) during peaks C and D $\delta^{13}C$ isotope excursions; this increase in abundance follows an overall decline in diversity and abundance of calcareous nannofossil assemblages (Figure 2). These changes, together with the absence of *Z. erectus* and *D. ignotus*, and a very low abundance of *Biscutum constans*, indicate a certain degree of diagenetic dissolution of nannofossil assemblages in the Youxia section.

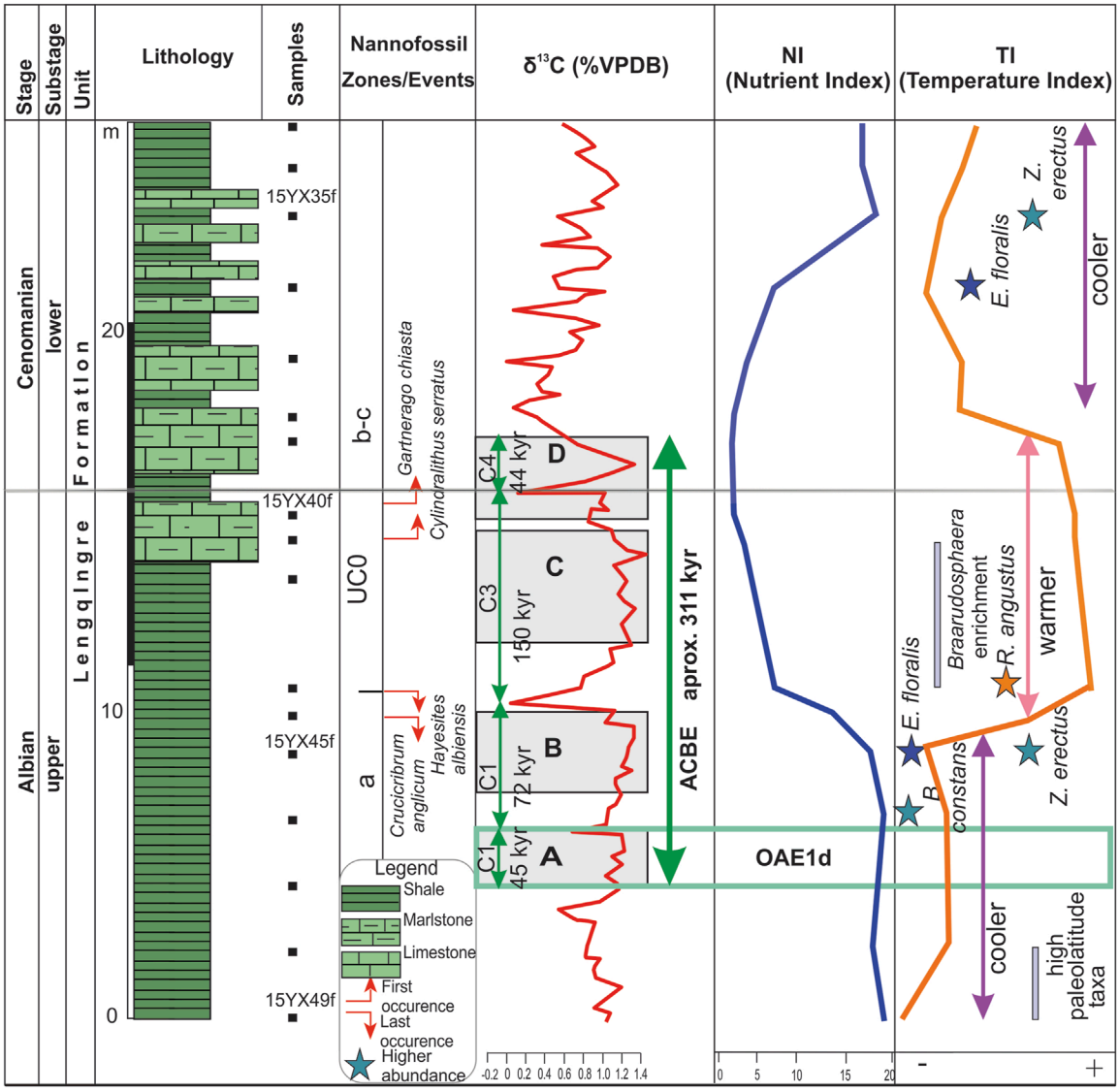

FIGURE 4
Fluctuation of NI (Nutrient Index), TI (Temperature Index), and main calcareous nannofossil events recorded in the studied section.

The calcareous nannofossil distribution pattern suggests that mesotrophic to eutrophic conditions were developed in the basin bellow, within, and slightly above the OAE1d event. The dominance of *W. barnesiae* may be indicative of an oligotrophic setting during the last phases of ACBE, but we may question if this is a real productivity signal or perhaps instead reflects diagenetic processes; this hypothesis is sustained by the occurrence of depauperate calcareous nannofossil assemblages that contain a small number of taxa, such as *W. barnesiae*, *E. floralis*, *Z. embergeri*, and *Rhagodiscus* spp., species known to be resistant to diagenetic dissolution (Erba et al., 2004; Erba, 2004; Lees et al., 2005).

In addition to the dominance of *W. barnesiae*, the late phases of ACBE are characterized by an increased abundance of *Braarudosphaera* taxa (*B. africana* and *B. hockwoldensis*) upwards of peak B and within peak C of $\delta^{13}C$. In general, taxa of the *Braarudosphaera* genus are rare throughout the Youxia section, except for this interval where they account for up to 15% of the assemblages, synchronous with the minimum in diversity and abundance of nannofossil assemblages.

It is worth noting that *Braarudosphaera* taxa are usually rare in the geological record, except for some 'critical intervals', such as OAE2 in the South Atlantic, Santos Basin, Brazil (Cunha and Shimabukuro, 1997), the Bohemian Basin, Czech Republic (Švábenická, 1999), the K/T boundary (i.e., Thierstein, 1980; Bown, 2005), and the Lower Oligocene deposits of the South Atlantic (Kelly et al., 2003). Nowadays, blooms of *Braarudosphaera bigelowii* are known to occur in the Black Sea, following the Holocene anoxic setting linked to the reconnection with the Mediterranean (Bukry et al., 1970; Giunta et al., 2007; Melinte-Dobrinescu and Ion, 2013; Briceag et al., 2019). Most probably, *Braarudosphaera* spp. are opportunistic taxa adapted to variable surface water conditions that include salinity and pH changes, which most probably occurred in association with the ACBE setting in the Youxia region.

In the studied section, the nannofossil assemblage recovery in abundance and diversity, characterized by higher abundance of *Biscutum constans* and *Z. erectus*, took place at 9.7 m above peak D, without reaching the values identified prior to and within the early phases of ACBE, i.e., OAE1d (Figure 2). Considering the average sedimentation rate of 7.18 cm/kyr at the Youxia section (Yao et al., 2018), it is probable that the recovery of nannofossil assemblages after the ACBE termination lasted around 140 Kyr.

Fluctuations of the NI (Nutrient Index) follow the calcareous nannofossil distribution and abundance patterns, as high values occur towards the base of the studied section with a maximum during OAE1d (peak A) and peak B, there is a sharp decrease in the ACBE later phases (peaks C and D), and then there is a recovery at the top of the studied succession (Figure 4). The NI index pattern shows that high productivity occurred below and during the early phases of the ACBE, with a progressive recovery of the surface water fertility well above the termination of the anoxic event in the early Cenomanian.

We may assume different causes for the two distinct episodes of higher productivity in the studied succession: the oldest one, developed in the early phases of the ACBE, is apparently triggered mainly by submarine volcanism, which might introduce abundant biolimiting metals in the ocean, while the youngest episode could be more related to the runoff following a warmer episode (as is indicated by the TI fluctuation).

5.2 Paleoenvironmental changes

Based on the TI fluctuation (Figure 4), a cooler climate mode is assumed for the lower part of the studied succession, extending over the early phases of the ACBE (peak A and the lower part of peak B of $\delta^{13}C$). The nannofossil assemblages of the above-mentioned interval include cosmopolitan taxa and a small group of species related to high paleolatitudes, such as *R. parvidentatum*, *S. primitivum*, and *S. horticus*, which are nannofossils reported from the Boreal areas of the Northern Hemisphere and Austral regions of the Southern Hemisphere (e.g., Mutterlose, 1992a; 1992b; Bown, 2001; Bornemann et al., 2017). The mixed nannofossil assemblages may indicate cooler water penetration from the south towards the Indian continental margin, where the study area is located, reflecting a transgressive event, i.e., the youngest and highest Albian eustatic event KAl8 (Haq, 2014).

An increased trend of TI, which indicates a warmer climate mode, was observed from the upper part of peak B, and continues in the youngest interval of ACBE with $\delta^{13}C$ positive excursions (peaks C and D) and slightly above. This assumption is based on the distribution pattern shown by several taxa considered to be significant proxies of paleoclimate changes, such as *E. floralis*, which decreases in abundance, and *Rhagodiscus angustus*, which shows higher values in the above-mentioned interval.

Eprolithus floralis is a species with higher abundance in the middle-to high paleolatitudes (Crux, 1991; Mutterlose et al., 2005; Bottini et al., 2015; Aguado et al., 2016, and references herein). Blooms of *E. floralis* are known to occur during anoxic events, i.e., OAE2, correlated with cooler climate intervals (e.g., Paul et al., 1999; Erba, 2004; Melinte-Dobrinescu et al., 2023). Conversely, the decline in *E. floralis* abundance concomitantly with higher $\delta^{13}C$ value intervals suggest warmer conditions during OAE2 (Hardas and Mutterlose, 2007).

In the Youxia section, distinctive enrichments of *E. floralis* were identified in the upper Albian, below the disappearance of *H. albiensis*, within $\delta^{13}C$ peak B and in the early Cenomanian, above the termination of ACBE. The oldest increase in abundance of *E. floralis* is coincident with the highest abundance of *Z. erectus*, while the youngest is situated slightly below *Z. erectus* enrichment. *Rhagodiscus angustus*, viewed as a warm surface water proxy (Roth and Krumbach, 1986; Erba et al., 1992; Herrle et al., 2003; Bottini and Erba, 2018), displays the highest abundance above peak B and continues to show high percentages upwards, within the youngest $\delta^{13}C$ peaks C and D of ACBE, starting to decrease after the termination of the anoxic event (Figures 2, 4). Overall, TI values indicate a cooler surface water interval in the late Albian, an increase of surface water temperature within the latest Albian-earliest Cenomanian, and the recurrence to a cooler climate mode in the early Cenomanian.

6 Conclusion

The calcareous nannofossil study from the Youxia Section, South Tibet, resulted in a comprehensive record of surface water temperature and productivity modifications in the Indian continental margin through the late Albian-early Cenomanian interval, including the ACBE. The calcareous nannofossil assemblages are generally composed of cosmopolitan and Tethyan taxa; the latter ones, including the nannoconids, show a low abundance and discontinuous occurrence throughout the whole studied succession. The only interval where nannofossils related to high paleolatitudes are present is the upper Albian, prior to the ACBE setting, in the UC0a subzone, below the LO of *C. anglicum*. The occurrence of mixed nannofossil assemblages is likely the result of a transgressive event whereby the oceanic circulation system led to cooler conditions associated with upwelling providing nutrient-rich waters, allowing the occurrence of assemblages including taxa with various paleobiogeographic affinities.

The changes in nannofossil assemblages, including the occurrence of high-fertility surface water proxies with higher abundance in two distinct intervals, i.e., early phases of ACBE (including OAE1d) and after the termination of ACBE, could be considered a primary paleoecological signal. By contrast, the significant decrease in nanofossil abundance and diversity during the late phases of ACBE, related to very high percentages of *W. barnesiae*, could be related to diagenetic processes, and might not reflect a decrease in productivity. Roth and Krumbach (1986), while studying mid-Cretaceous sediments of the Atlantic and Indian oceans, concluded that a significant organic carbon content in sedimentary deposits may affect the preservation of nannofossils. Thus, we hypothesize that a significant rise in atmospheric CO_2 occurred in the late phases of ACBE in the studied region, leading to higher dissolved carbon dioxide content and changing the physical and chemical parameters of the surface waters. This process led to a temporary disappearance of some nannofossils, particularly those receptive to the diagenesis; however, a decrease in the primary productivity could also have occurred in the late phases of ACBE.

Variations in the temperature and nutrient indices show both similar and opposite trends on various intervals of the studied succession. This pattern reveals that the two indices were

mostly independent of each other, or they do not reflect the original paleoecological signal, especially in the depositional intervals containing nannofossil assemblages affected by diagenetic processes. A good correlation between TI and NI in the lower part of the succession, i.e., prior to OAE1d and in the early phases of ACBE, is indicative of a temperature decrease in the surface waters, accompanied by increased productivity. These changes possibly reflect the ocean circulation modifications in the Southern Hemisphere resulting from the enhanced connection among different oceanic basins during the mid-Cretaceous.

The results provided by this work suggest similarities between western and eastern Tethyan domains concerning the biostratigraphy and distribution of the calcareous nannofossils, including the existence of a nutrification episode associated with OAE1d (Bornemann et al., 2005; Bornemann and Mutterlose, 2006; Bottini and Erba, 2018; Bąk et al., 2023 and references herein). The distribution pattern of nannofossils indicates major changes during the ACBE, including fluctuations of temperature, nutrient amount, and pH values related to a global anoxic event with a specific overprint due to the regional setting of the Indian continental margin.

Data availability statement

The raw data supporting the conclusions of this article will be made available by the authors, without undue reservation.

Author contributions

MM-D: Investigation, Methodology, Writing–original draft, Conceptualization, Data curation, Writing–review and editing. XC: Investigation, Writing–original draft. EA: Formal Analysis, Writing–original draft. VA: Conceptualization, Writing–original draft. HY: Investigation, Writing–review and editing.

Funding

The author(s) declare that financial support was received for the research, authorship, and/or publication of this article. This work was supported by the Project of the Romanian Agency of Education and Research CNCS-UEFSCDI, project number PN-III-P4-ID-PCE-2021-0901 – DEVOBAS and Project PNRR C9 - I8, code 97/15.11.2022, Contract No. 760115/23.05.2023.

Acknowledgments

The authors thank the reviewers and the Guest Editor Florentin Maurrasse, whose comments substantially improved an earlier version of this paper.

Conflict of interest

The authors declare that the research was conducted in the absence of any commercial or financial relationships that could be construed as a potential conflict of interest.

Publisher's note

Supplementary material

The Supplementary Material for this article can be found online at: https://www.frontiersin.org/articles/10.3389/feart.2024.1405768/full#supplementary-material

SUPPLEMENTARY TABLE S1
Distribution chart of the identified calcareous nannofossils in the Youxia section (S Tibet). P (present) = 1–3/specimens/8 FOVs; R (rare) = 1–3 specimens/5 FOVs; F (few) = 4–7 specimens/5 FOVs; C (common) = 7–10 specimens/5 FOVs; A (abundant) = >10 specimens/5 FO.

References

Aguado, R., Reolid, M., and Molina, E. (2016). Response of calcareous nannoplankton to the Late Cretaceous Oceanic Anoxic Event 2 at Oued Bahloul (central Tunisia). *Palaeogeogr. Palaeoclim. Palaeoecol.* 459, 289–305. doi:10.1016/j.palaeo.2016.07.016

Applegate, J. L., and Bergen, J. A. (1988). Cretaceous calcareous nannofossil biostratigraphy of sediments recovered from the Galicia Margin, ODP Leg 103. *Proc. Odp. Sci. Results* 103, 293–348.

Arthur, M. A., Dean, W. E., and Pratt, L. M. (1988). Geochemical and climatic effects of increased marine organic carbon burial at the Cenomanian/Turonian boundary. *Nature* 335, 714–717. doi:10.1038/335714a0

Arthur, M. A., Dean, W. E., and Schlanger, S. O. (1985). "Variations in the global carbon cycle during the Cretaceous related to climate, volcanism, and changes in atmospheric CO_2," in *The carbon cycle and atmospheric CO_2: natural variations Archean to Present*. Editors E. T. Sundquist, and W. S. Broecker (Washington D.C.: Geophys. Monogr. Ser.), 504–529.

Arthur, M. A., and Premoli Silva, I. (1982). "Development of widespread organic carbon-rich strata in the Mediterranean Tethys," in *Nature and origin of Cretaceous carbon-rich facies*. Editors S. O. Schlanger, and M. B. Cita (London: Acad. Press), 7–54.

Bąk, K., Szram, E., Zielińska, M., Misz-Kennan, M., Fabiánska, M., Bąk, M., et al. (2023). Organic matter variations in the deep marginal basin of the Western Tethys and links to various environments in isotopic Albian–Cenomanian Boundary Interval. *Int. J. Coal Geol.* 266, 104181. doi:10.1016/j.coal.2022.104181

Bodin, S., Krencker, F.-N., Kabiri, L., and Immenhauser, A. (2015). The Toarcian Oceanic Anoxic Event: a shallow-water perspective. EGU general assembly conference 2015. *geophys. Res. Abstr.* 17. EGU2015-3398.

Bodin, S., Mattioli, E., Fröhlich, S., Marshall, J. D., Boutib, L., Lahsini, S., et al. (2010). Toarcian carbon isotope shifts and nutrient changes from the northern margin of Gondwana (High Atlas, Morocco, Jurassic): palaeoenvironmental implications. *Palaeogeogr. Palaeoclimatol. Palaeoecol.* 297 (2), 377–390. doi:10.1016/j.palaeo.2010.08.018

Bornemann, A., Erbacher, J., Heldt, M., Kollaske, T., Wilmsen, M., Lübke, N., et al. (2017). The Albian-Cenomanian transition and Oceanic Anoxic Event 1d – an example from the Boreal Realm. *Sedimentology* 64, 44–65. doi:10.1111/sed.12347

Bornemann, A., and Mutterlose, J. (2006). Size analyses of the coccolith species *Biscutum constans* and *Watznaueria barnesiae* from the Late Albian "Niveau Breistroffer" (SE France): taxonomic and palaeoecological implications. *Geobios* 39 (5), 599–615. doi:10.1016/j.geobios.2005.05.005

Bornemann, A., Pross, J., Reichelt, K., Herrle, J. O., Hemleben, C., and Mutterlose, J. (2005). Reconstruction of short-term palaeoceanographic changes during the Formation of the late Albian 'Niveau Breistroffer' black shales (oceanic anoxic event 1d, SE France). *J. Geol. Soc.* 162 (4), 623–639. doi:10.1144/0016-764903-171

Bottini, C., and Erba, E. (2018). Mid-Cretaceous paleoenvironmental changes in the western Tethys. *Clim. Past.* 14 (8), 1147–1163. doi:10.5194/cp-14-1147-2018

Bottini, C., Erba, E., Tiraboschi, D., Jenkyns, H. C., Schouten, S., and Sinninghe Damsté, J. S. (2015). Climate variability and ocean fertility during the Aptian Stage. *Clim. Past.* 11, 383–402. doi:10.5194/cp-11-383-2015

Bown, P. R. (2001). Calcareous nannofossils of the Gault, Upper Greensand and Glauconitic Marl (Middle Albian-Lower Cenomanian) from the BGS Selborne boreholes, Hampshire. *Proc. Geol. Assoc.* 112, 223–236. doi:10.1016/S0016-7878(01)80003-1

Bown, P. R. (2005). Selective calcareous nannoplankton survivorship at the Cretaceous–Tertiary boundary. *Geology* 33, 653–656. doi:10.1130/G21566AR.1

Bown, P. R., Rutledge, D. C., Crux, J. A., and Gallagher, L. T. (1998). "Lower Cretaceous", in P. R. Bown (Ed.), *Calcareous nannofossil biostratigraphy*. British Micropalaeontological Society Publication Series. Chapman and Hall Ltd/Kluwer Academic Press, Kluwer Academic Publishers, Dordrecht, Boston, London, 86–131.

Bown, P. R., and Young, J. R. (1998). "Techniques," in *Calcareous nannofossil biostratigraphy*. Editor P. R. Bown (Dordrecht, Boston, London: British Micropalaeontological Society Publication Series. Chapman and Hall Ltd/Kluwer Academic Press, Kluwer Academic Publishers), 16–28.

Bréhéret, J.-G. (1997). L'Aptien et l'Albien de la Fosse Vocontienne (bordures et basin): Évolution de la sedimentation et enseignements sur les événements anoxiques. *Publ. Soc. Geol. Nord.* 25, 614.

Breistroffer, M., and Hebd, C. R. (1937). Sur les niveaux fossilifères de l'Albien dans la fosse vocontienne (Drôme, Hautes-Alpes et Basses Alpes). *Seances Acad. Sci. Ser. D.* 204, 1492–1493.

Briceag, A., Yanchilina, A., Ryan, W. B. F., Stoica, M., and Melinte-Dobrinescu, M. C. (2019). Late Pleistocene to Holocene paleoenvironmental changes in the NW Black Sea. *J. Quat. Sci.* 34 (2), 87–100. doi:10.1002/jqs.3083

Bruno, M. D. R., Fauth, G., Watkins, D. K., Goulart, M., Caramez, M. G. S., Nauter-Alves, A., et al. (2022). Paleoceanographic evolution in the South Atlantic Ocean (Kwanza Basin, Angola) during its post-salt foundering. *Mar. Petrol. Geol.* 144, 105852. doi:10.1016/j.marpetgeo.2022.105852

Bukry, D. (1974). "Coccoliths as paleosalinity indicators – evidence from Black Sea," in *The Black Sea – geology, chemistry and biology. Mem. Am. Assoc petrol. Geol.* Editors E. T. Degens, and D. A. Ross, 20, 353–363.

Bukry, D., King, A. S., Horn, M. K., and Manheim, F. T. (1970). Geological significance of coccoliths in fine-grained carbonate bands of postglacial Black Sea sediments. *Nature* 26 (5241), 156–158. doi:10.1038/226156a0

Burnett, J. (1998). "Upper Cretaceous calcareous nannofossil biostratigraphy," in *Calcareous nannofossil biostratigraphy*. Editor P. R. Bown (Dordrecht, Boston, London: British Micropalaeontological Society Publication Series. Chapman and Hall Ltd/Kluwer Academic Press, Kluwer Academic Publishers), 132–199.

Chin, S. K., and Watkins, D. K. (2019). "Paleoecological response of calcareous nannofossils during the Albian–Cenomanian boundary and Early Cenomanian events at deep sea drilling project hole 547a, northwestern African margin," in *Geologic problem solving with microfossils IV. Soc. Sedim. Geol.* Editors R. A. Denne, and A. Kahn, 111. doi:10.2110/sepmsp.111

Coccioni, R., Luciani, V., and Marsili, A. (2006). Cretaceous oceanic anoxic events and radially elongated chambered planktonic foraminifera: paleoecological and paleoceanographic implications. *Palaeogeogr. Palaeoclimatol. Palaeoecol.* 235 (1–3), 66–92. doi:10.1016/j.palaeo.2005.09.024

Cohen, A. S., Coe, A. L., and Kemp, D. B. (2007). The Late Palaeocene–Early Eocene and Toarcian (Early Jurassic) carbon isotope excursions: a comparison of their time scales, associated environmental changes, causes and consequences. *J. Geol. Soc.* 164, 1093–1108. doi:10.1144/0016-76492006-123

Crux, J. A. (1991). Albian calcareous nannofossils from the Gault clay of Munday's Hill (Bedfordshire, England). *Journ. Micropal.* 10 (2), 203–221. doi:10.1144/jm.10.2.203

Cunha, A. S., and Shimabukuro, S. (1997). *Braarudosphaera* blooms and anomalous enrichments of Nannoconus: evidence from the Turonian south Atlantic, Santos basin, Brazil. *JNR* 19, 51–55.

Dumitrescu, M., and Brassell, S. C. (2006). Compositional and isotopic characteristics of organic matter for the early Aptian oceanic anoxic event at Shatsky Rise, ODP Leg 198. *Palaeogeogr. Palaeoclimatol. Palaeoecol.* 235, 168–191. doi:10.1016/j.palaeo.2005.09.028

Erba, E. (2004). Calcareous nannofossils and Mesozoic oceanic anoxic events. *Mar. Micropaleontol.* 52 (1–4), 85–106. ISSN 0377-8398. doi:10.1016/j.marmicro.2004.04.007

Erba, E., Bartolini, A., and Larson, R. L. (2004). Valanginian Weissert oceanic anoxic event. *Geology* 32, 149–152. doi:10.1130/G20008.1

Erba, E., Castradori, D., Guasti, G., and Ripepe, M. (1992). Calcareous nannofossils and Milankovitch cycles: the example of the Albian Gault clay formation (southern England). *Palaeogeogr. Palaeoclimatol. Palaeoecol.* 93, 47–69. doi:10.1016/0031-0182(92)90183-6

Erba, E., and Tremolada, F. (2004). Nannofossil carbonate fluxes during the Early Cretaceous: phytoplankton response to nutrification episodes, atmospheric CO_2, and anoxia. *Paleoceanogr* 19, PA1008. doi:10.1029/2003PA000884

Fahdel, M. B., Layeb, M., Hedfi, Y., and Youssed, M. B. (2011). Albian oceanic anoxic events in northern Tunisia: biostratigraphic and geochemical insights. *Cretac. Res.* 32 (6), 685–699. doi:10.1016/j.cretres.2011.04.004

Fan, Q., Xu, Z., MacLeod, K. G., Brumsack, H.-J., Li, T., Chang, F., et al. (2022). First record of oceanic anoxic event 1d at Southern high latitudes: sedimentary and geochemical evidence from International Ocean Discovery Program Expedition 369. *Geophys. Res. Lett.* 49, e2021GL097641. doi:10.1029/2021GL097641

Föllmi, K. B., Weissert, H., Bisping, M., and Funk, H. (1994). Phosphogenesis, carbon-isotope stratigraphy, and carbonate platform evolution along the Lower Cretaceous northern Tethyan margin. *GSA Bull.* 106 (6), 729–746. doi:10.1130/0016-7606(1994)106<0729:PCISAC>2.3.CO;2

Frey, F. A., Coffin, M. F., Wallace, P. J., Weis, D., Zhao, X., Wise, Jr., S. W., et al. (2000). Origin and evolution of a submarine large igneous province: the Kerguelen Plateau and Broken Ridge, southern Indian Ocean. *Earth Planet. Sci. Lett.* 176, 73–89. doi:10.1016/S0012-821X(99)00315-5

Friedrich, O., Norris, R. D., and Erbacher, J. (2012). Evolution of middle to Late Cretaceous oceans – a 55 m.y. record of Earth's temperature and carbon cycle. *Geology* 40 (568), 107–110. doi:10.1130/G32701.1

Gale, A. S., Bown, P., Caron, M., Crampton, J., Crowhurst, S. J., Kennedy, W. J., et al. (2011). The uppermost Middle and Upper Albian succession at the Col de Palluel, Hautes-Alpes, France: An integrated study (ammonites, inoceramid bivalves, planktonic foraminifera, nannofossils, geochemistry, stable oxygen, and carbon isotopes, cyclostratigraphy). *Cretac. Res.* 32 (2), 59–130. ISSN 0195-6671. doi:10.1016/j.cretres.2010.10.004

Gale, A. S., Kennedy, W. J., Burnett, J. A., Caron, M., and Kidd, B. E. (1996). The Late Albian to Early Cenomanian succession at Mont Risou near Rosans (Drôme, SE France): an integrated study (ammonites, inoceramids, planktonic foraminifera, nannofossils, oxygen and carbon isotopes). *Cretac. Res.* 17, 515–606. doi:10.1006/cres.1996.0032

Gambacorta, G., Jenkyns, H. C., Russo, F., Tsikos, H., Wilson, P. A., Faucher, G., et al. (2015). Carbon- and oxygen-isotope records of mid-Cretaceous Tethyan pelagic sequences from the Umbria-Marche and Belluno Basins (Italy). *Newsl. Stratigr.* 48, 299–323. doi:10.1127/nos/2015/0066

Gansser, A. (1991). Facts and theories on the Himalayas. *Eclog. Geol. Helv.* 84 (1), 33–59.

Giraud, F., Olivero, D., Baudin, F., Reboulet, S., Pittet, B., and Proux, O. (2003). Minor changes in surface-water fertility across the oceanic anoxic event 1d (latest Albian, SE France) evidenced by calcareous nannofossils. *Int. J. Earth Sci.* 92, 267–284. doi:10.1007/s00531-003-0319-x

Giunta, S., Morigi, C., Negri, A., Guichard, F., and Lericolais, G. (2007). Holocene biostratigraphy and paleoenvironmental changes in the Black Sea based on calcareous nannoplankton. *Mar. Micropaleontol.* 63, 91–110. doi:10.1016/j.marmicro.2006.12.001

Górny, Z., Bąk, M., Bąk, K., and Strzeboński, P. (2022). Planktonic biota constituents responses to global sea-level changes recorded in the uppermost Albian to middle Cenomanian deep-water facies of the outer Carpathians. *Minerals* 12 (2), 152. doi:10.3390/min12020152

Haq, B. U. (2014). Cretaceous eustasy revisited. *Glob. Planet. Change* 113, 44–58. doi:10.1016/j.gloplacha.2013.12.007

Hardas, P., and Mutterlose, J. (2007). Calcareous nannofossil assemblages of Oceanic Anoxic Event 2 in the equatorial Atlantic: evidence of an eutrophication event. *Mar. Micropaleontol.* 66, 52–69. doi:10.1016/j.marmicro.2007.07.007

Hay, W. W. (2009). "Cretaceous oceans and ocean modeling," in *Cretaceous oceanic red beds: stratigraphy, composition, origins, and paleoceanographic and paleoclimatic significance*. Editors X. Hu, C. Wang, R. W. Scott, M. Wagreich, and L. Jansa (Tulsa, Oklahoma: SEPM Sp), 243–271. Publ. 91.

Herrle, J. O., and Mutterlose, J. (2003). Calcareous nannofossils from the Aptian–Lower Albian of southeast France: palaeoecological and biostratigraphic implications. *Cretac. Res.* 24 (1), 1–22. doi:10.1016/S0195-6671(03)00023-5

Herrle, J. O., Pross, J., Friedrich, O., Kössler, P., and Hemleben, C. (2003). Forcing mechanisms for Mid-Cretaceous black shale formation: evidence from the upper Aptian and lower Albian of the Vocontian Basin (SE France). *Palaeogeogr. Palaeoclim. Palaeoecol.* 190, 399–426. doi:10.1016/S0031-0182(02)00616-8

Hu, X., Jansa, L., Chen, L., Gri-ffin, W. L., O'Reilly, S. Y., and Wang, J. (2010). Provenance of Lower Cretaceous Wölong volcaniclastics in the Tibetan Tethyan Himalaya: implications for the final breakup of eastern gondwana. *Sediment. Geol.* 223, 193–205. doi:10.1016/j.sedgeo.2009.11.008

Huber, B. T., MacLeod, K. G., Watkins, D. K., and Coffin, M. F. (2018). The rise and fall of the Cretaceous hot greenhouse climate. *Glob. Planet. Change* 167, 1–23. doi:10.1016/j.gloplacha.2018.04.004

Ion, G., Briceag, A., Vasiliu, D., Lupaşcu, N., and Melinte-Dobrinescu, M. (2022). A multiproxy reconstruction of Late Pleistocene-Holocene paleoenvironment: new insights from the NW Black Sea. *Mar. Geol.* 443, 1066448. doi:10.1016/j.margeo.2021.106648

Jarvis, I., Gale, A. S., Jenkyns, H. G., and Pearch, M. A. (2006). Secular variation in Late Cretaceous carbon isotopes: a new $\delta^{13}C$ carbonate reference curve for the Cenomanian–Campanian (99.6–70.6 Ma) Cretaceous carbon isotopes: a new $\delta^{13}C$ carbonate reference curve for the Cenomanian–Campanian (99.6–70.6 Ma). *Geol. Mag.* 143 (5), 561–608. doi:10.1017/S0016756806002421

Jenkyns, H. C. (1980). Cretaceous anoxic events: from continents to oceans. *J. Geol. Soc.* 137, 171–188. doi:10.1144/gsjgs.137.2.0171

Jenkyns, H. C. (2010). Geochemistry of oceanic anoxic events. *Geochem. Geophys.* 11 (3). doi:10.1029/2009GC002788

Jenkyns, H. C., and Clayton, C. J. (1986). Black shales and carbon isotopes in pelagic sediments from the Tethyan Lower Jurassic. *Sedimentology* 33, 87–106. doi:10.1111/j.1365-3091.1986.tb00746.x

Jenkyns, H. C., Dickson, A. J., Ruhl, M., and Boorn, S. H. (2017). Basalt-seawater interaction, the Plenus Cold Event, enhanced weathering, and geochemical change: deconstructing Oceanic Anoxic Event 2 (Cenomanian–Turonian, Late Cretaceous). *Sedimentology* 64 (1), 16–43. doi:10.1111/sed.12305

Jenkyns, H. C., Gale, A. S., and Corfield, R. M. (1994). Carbon- and oxygen-isotope stratigraphy of the English Chalk and Italian Scaglia and its palaeoclimatic significance. *Geol. Mag.* 131, 1–34. doi:10.1017/S0016756800010451

Jeremiah, J. (1996). A proposed Albian to Lower Cenomanian nannofossil biozonation for England and the North Sea Basin. *J. Micropalaeontol.* 15, 97–129. doi:10.1144/jm.15.2.97

Jiang, S., Jiang, Y., Liu, Y., Li, S., Zhang, W., Wang, G., et al. (2021). The Bangong-Nujiang suture zone, Tibet plateau: its role in the tectonic evolution of the eastern Tethys Ocean. *Earth-Sci. Rev.* 2018, 103656. doi:10.1016/j.earscirev.2021.103656

Kelly, D. C., Norris, R. D., and Zachos, J. C. (2003). Deciphering the paleoceanographic significance of Early Oligocene *Braarudosphaera* chalks in the South atlantic. *Mar. Micropaleontol.* 49, 49–63. doi:10.1016/s0377-8398(03)00027-6

Kemp, D. B., Suan, G., Fantasia, A., Jin, S., and Chen, W. (2022). Global organic carbon burial during the Toarcian oceanic anoxic event: patterns and controls. *Earth-Sci. Rev.* 231, 104086. doi:10.1016/j.earscirev.2022.104086

Kennedy, W. J., Gale, A. S., Lees, J. A., and Caron, M. (2004). The global boundary stratotype section and point (GSSP) for the base of the Cenomanian stage, Mont Risou, Hautes-Alpes, France. *Episodes* 27 (1), 21–32. doi:10.18814/epiiugs/2004/v27i1/003

Kuypers, M. M. M., Pancost, R. D., and Sinninghe Damsté, J. S. (1999). A large and abrupt fall in atmospheric CO2 concentration during Cretaceous times. *Nature* 399, 342–345. doi:10.1038/20659

Lamolda, M. A., Gorostidi, A., and Paul, C. R. C. (1994). Quantitative estimates of calcareous nannofossil changes across the Plenus Marls (latest Cenomanian), Dover, England: implications for the generation of the Cenomanian-Turonian boundary event. *Cretac. Res.* 14, 143–164. doi:10.1006/cres.1994.1007

Larson, R. L. (1991). Latest pulse of Earth: evidence for a mid-Cretaceous superplume. *Geology* 19 (6), 547–550. doi:10.1130/0091-7613(1991)019<0547:lpoeef>2.3.co;2

Larson, R. L., and Erba, E. (1999). Onset of the Mid-Cretaceous greenhouse in the Barremian-Aptian: igneous events and the biological, sedimentary, and geochemical responses. *Paleoceanogr* 14 (6), 663–678. doi:10.1029/1999PA900040

Leckie, R. M., Bralower, T. J., and Cashman, R. (2002). Oceanic anoxic events and plankton evolution: biotic response to tectonic forcing during the mid-Cretaceous. *Paleoceanogr* 17 (3), 1041. doi:10.1029/2001PA000623

Lees, J. A., Bown, P. R., and Mattioli, E. (2005). Problems with proxies? Cautionary tales of calcareous nannofossil paleoenvironmental indicators. *Micropaleontology* 51 (4), 333–343. doi:10.2113/gsmicropal.51.4.333

Li, X., Jenkyns, H. C., Wang, C., Hu, X., Chen, X., Wei, Y., et al. (2006). Upper Cretaceous carbon- and oxygen-isotope stratigraphy of hemipelagic carbonate facies from southern Tibet, China. *J. Geol. Soc.* 163, 375–382. doi:10.1144/0016-764905-046

Linnert, C., Mutterlose, J., and Erbacher, J. (2010). Calcareous nannofossils of the Cenomanian/Turonian boundary interval from the boreal Realm (Wunstorf, northwest Germany). *Mar. Micropaleontol.* 74, 38–58. doi:10.1016/j.marmicro.2009.12.002

Mansour, A., and Wagreich, M. (2024). An overview of the Cretaceous oceanic anoxic events in Egypt, southern Tethys. *Geol. Soc. Spec. Publ.* 545. doi:10.1144/SP545-2023-104

McAnena, A., Flögel, S., Hofmann, P., Herrle, J. O., Griesand, A., Pross, J., et al. (2013). Atlantic cooling associated with a marine biotic crisis during the mid-Cretaceous period. *Nat. Geosci.* 6, 558–561. doi:10.1038/ngeo1850

Melinte, M., and Mutterlose, J. (2001). A Valanginian (Early Cretaceous) 'boreal nannoplankton excursion' in sections from Romania. *Mar. Micropaleontol.* 45, 1–25. doi:10.1016/S0377-8398(01)00022-6

Melinte-Dobrinescu, M., and Ion, G. (2013). *Emiliania huxleyi* fluctuations and associated microalgae in superficial sediments of the Romanian Black Sea Shelf. *Geo-Eco-Marina* 13, 129135. doi:10.5281/zenodo.56850

Melinte-Dobrinescu, M. C., Bernández, E., Kaiho, K., and Lamolda, M. A. (2013). Cretaceous Oceanic Anoxic Event 2 in the Arobes section, northern Spain: calcareous nannofossil fluctuations and isotopic events. *J. Geol. Soc. Lond.* 382, 8298. doi:10.1144/SP382.7

Melinte-Dobrinescu, M. C., Ion, G., Anton, E., Apostrosoaei, V., Briceag, A., and Lazăr, C. (2023). First record of Oceanic Anoxic Event 2 in the Eastern Carpathians: implications for chemostratigraphic and biostratigraphic correlations. *Front. Earth Sci.* 11, 1155482. doi:10.3389/feart.2023.1155482

Melinte-Dobrinescu, M. C., Roban, R.-D., and Stoica, M. (2015). Palaeoenvironmental changes across the Albian-Cenomanian boundary interval of the eastern Carpathians. *Cretac. Res.* 54 (1), 68–85. doi:10.1016/j.cretres.2014.10.010

Menegatti, A. P., Weissert, H., Brown, R. S., Tyson, R. V., Farrimond, P., Strasser, A., et al. (1998). High resolution $\delta^{13}C$-stratigraphy through the early Aptian "livello selli" of the alpine Tethys. *Paleoceanogr* 13 (5), 530–545. doi:10.1029/98PA01793

Mitchell, S., Paul, C., and Gale, A. (1996). Carbon isotopes and sequence stratigraphy. *Geol. Soc. Spec. Publ.* 104, 11–24. doi:10.1144/GSL.SP.1996.104.01.02

Mutterlose, J. (1992a). Migration and evolution patterns of floras and faunas in marine Early Cretaceous sediments of NW Europe. *Palaeogeogr. Palaeoclim. Palaeoecol.* 94, 261–282. doi:10.1016/0031-0182(92)90123-m

Mutterlose, J. (1992b). Lower Cretaceous nannofossil biostratigraphy off northwestern Australia (Leg 123). *Proc. Odp. Sci. Res.* 123, 343–368.

Mutterlose, J., Bornemann, A., and Herrle, J. O. (2005). Mesozoic calcareous nannofossils - state of the art. *Paläontol. Z.* 79 (1), 113–133. doi:10.1007/bf03021757

Mutterlose, J., and Kessels, K. (2000). Early Cretaceous calcareous nannofossils from high latitudes: implications for palaeobiogeography and palaeoclimate. *Palaeogeogr. Palaeoclimatol. Palaeoecol.* 160, 347–372. doi:10.1016/s0031-0182(00)00082-1

Mutterlose, J., Klopschar, M., and Visentin, S. (2022). Ecological adaptation of marine floras and faunas across the Early Jurassic Toarcian Oceanic Anoxic Event – a case study from northern Germany. *Palaeogeogr. Palaeoclimatol. Palaeoecol.* 602, 111176. doi:10.1016/j.palaeo.2022.111176

Patzelt, A., Li, H., Wang, J., and Appel, E. (1996). Palaeomagnetism of Cretaceous to Tertiary sediments from southern Tibet: evidence for the extent of the northern margin of India prior to the collision with Eurasia. *Tectonophysics* 259, 259–284. doi:10.1016/0040-1951(95)00181-6

Paul, C. R. C., Lamolda, M. A., Mitchell, S. F., Vaziri, M. R., Gorostidi, A., and Marshall, J. D. (1999). The Cenomanian–Turonian boundary at Eastbourne (Sussex, UK): a proposed European reference section. *Palaeoecol* 150, 83–121. doi:10.1016/S0031-0182(99)00009-7

Petrizzo, M. R., Huber, B. T., Wilson, P. A., and MacLeod, K. G. (2008). Late Albian paleoceanography of the western subtropical North Atlantic. *Paleoceanography* 23 (1-17). PA1213. doi:10.1029/2007PA001517

Richey, J. D., Upchurch, G. R., Montañez, I. P., Lomax, B. H., Suarez, M. B., Crout, M. J. N., et al. (2018). Changes in CO_2 during ocean anoxic event 1d indicate similarities to other carbon cycle perturbations. *Earth Planet. Sci. Lett.* 491, 172–182. doi:10.1016/j.epsl.2018.03.035

Roth, P. H., and Krumbach, K. R. (1986). Middle Cretaceous calcareous nannofossil biogeography and preservation in the Atlantic and Indian oceans: implications for paleoceanography. *Mar. Micropaleontol.* 10, 235–266. doi:10.1016/0377-8398(86)90031-9

Sames, B., Wagreich, M., Wendler, J. E., Haq, B. U., Conrad, C. P., Melinte-Dobrinescu, M. C., et al. (2016). Review: short-term sea-level changes in a greenhouse world — a view from the Cretaceous. *Palaeogeogr. Palaeoclimatol. Palaeoecol.* 441, 393–411. doi:10.1016/j.palaeo.2015.10.045

Schlanger, S. O., and Jenkyns, H. C. (1976). Cretaceous oceanic anoxic events: causes and consequences. *Geol. Mijnb.* 55, 179–184.

Scotese, C. (1991). Jurassic and Cretaceous plate tectonic reconstructions. *Palaeogeogr. Palaeoclimatol. Palaeoecol.* 87, 493–501. doi:10.1016/0031-0182(91)90145-H

Scotese, C. (2021). An Atlas of Phanerozoic Paleogeographic Maps: the seas come in and the seas go out. *Annu. Rev. Earth Planet. Sci.* 49 (1), 679–728. doi:10.1146/annurev-earth-081320-064052

Scott, R. W., Formolo, M., Rush, N., Owens, J. D., and Oboh-Ikuenobe, F. (2013). Upper Albian OAE 1d event in the Chihuahua Trough, New Mexico, U.S.A. *Cretac. Res.* 46, 136–150. doi:10.1016/j.cretres.2013.08.011

Street, C., and Bown, P. R. (2000). Palaeobiogeography of Early Cretaceous (Berriasian–Barremian) calcareous nannoplankton. *Mar. Micropalaeontol.* 39, 265–291. doi:10.1016/S0377-8398(00)00024-4

Švábenická, L. (1999). *Braarudosphaera*-rich sediments in the Turonian of the Bohemian Cretaceous Basin, Czech Republic. *Cretac. Res.* 20, 773–782. doi:10.1006/cres.1999.0182

Thierstein, H. R. (1980). Selective dissolution of Late Cretaceous and Earliest Tertiary calcareous nannofossils: experimental evidence. *Cretac. Res.* 2, 165–176. doi:10.1016/0195-6671(80)90023-3

Tiraboschi, D., Erba, E., and Jenkyns, H. C. (2009). Origin of rhythmic Albian black shales (Piobbico core, central Italy): Calcareous nannofossil quantitative and statistical analyses and paleoceanographic reconstructions. *Paleoceanogr* 24, PA2222. doi:10.1029/2008PA001670

Turgeon, S., and Brumsack, H.-J. (2006). Anoxic vs dysoxic events reflected in sediment geochemistry during the Cenomanian–Turonian Boundary Event (Cretaceous) in the Umbria–Marche Basin of central Italy. *Chem. Geol.* 234 (3–4), 321–339. doi:10.1016/j.chemgeo.2006.05.008

Wang, Y., Bodin, S., Blusztajn, J. S., Ullmann, C., and Nielsen, S. G. (2022). Orbitally paced global oceanic deoxygenation decoupled from volcanic CO_2 emission during the middle Cretaceous Oceanic Anoxic Event 1b (Aptian-Albian transition). *Geology* 50 (11), 1324–1328. doi:10.1130/G50553.1

Weissert, H., and Erba, E. (2004). Volcanism, CO2 and palaeoclimate: a Late Jurassic–Early Cretaceous carbon and oxygen isotope record. *J. Geol. Soc. Lond.* 161 (4), 695–702. doi:10.1144/0016-764903-087

Willems, H., Zhou, Z., Zhang, B., and Grafe, K.-U. (1996). Stratigraphy of the Upper Cretaceous and Lower Tertiary strata in the Tethyan Himalayas of Tibet (Tingri area, China). *Geol. Rundsch.* 85 (4), 723. doi:10.1007/bf02440107

Wilson, P. A., and Norris, R. D. (2001). Warm tropical ocean surface and global anoxia during the mid-Cretaceous period. *Nature* 412, 425–429. doi:10.1038/35086553

Yao, H., Chen, X., Melinte-Dobrinescu, M. C., Wu, H., Liang, H., and Weissert, H. (2018). Biostratigraphy, carbon isotopes and cyclostratigraphy of the Albian-Cenomanian transition and Oceanic Anoxic Event 1d in southern Tibet. *Palaeogeogr. Palaeoclimatol. Palaeoecol.* 499, 45–55. doi:10.1016/j.palaeo.2018.03.005

Yao, H., Chen, X., Yin, R., Grasby, S. E., Weissert, H., Gu, X., et al. (2021). Mercury evidence of intense volcanism preceded oceanic anoxic event 1d. *Geophys. Res. Lett.* 48 (5), e2020GL091508. doi:10.1029/2020GL091508

Yilmaz, İ. Ö. (2008). Cretaceous pelagic red beds and black shales (Aptian – Santonian), NW Turkey: Global Oceanic Anoxic and Oxic Events. *Turk. J. Earth Sci.* 17 (2), 263–296.